Published in final edited form as:
J Magn Reson Imaging. 2008 July ; 28(1): 80–88. doi:10.1002/jmri.21408.

Assessment of the lung microstructure in patients with asthma using hyperpolarized ^{3}He diffusion MRI at two time scales: Comparison with healthy subjects and patients with COPD

Chengbo Wang, PhD[1,*], **Talissa A. Altes, MD**[1], **John P. Mugler III, PhD**[1,2], **G. Wilson Miller, PhD**[1], **Kai Ruppert, PhD**[1,3], **Jaime F. Mata, PhD**[1], **Gordon D. Cates Jr, PhD**[1,4], **Larry Borish, MD**[5], and **Eduard E. de Lange, MD**[1]

[1]Department of Radiology, University of Virginia, Charlottesville, Virginia, USA

[2]Department of Biomedical Engineering, University of Virginia, Charlottesville, Virginia, USA

[3]Department of Radiology, Children's Hospital of Philadelphia, Philadelphia, Pennsylvania, USA

[4]Departments of Physics, University of Virginia, Charlottesville, Virginia, USA

[5]Department of Medicine, Allergy and Immunology, University of Virginia, Charlottesville, Virginia, USA

Abstract

Purpose—To investigate short- and long-time-scale ^{3}He diffusion in asthma.

Materials and methods—A hybrid MRI sequence was developed to obtain co-registered short- and long-time-scale ADC maps during a single breath-hold. Study groups: asthma (n=14); healthy (n=14); COPD (n=9). Correlations were made between mean-ADC and %ADC-abn (%pixels with ADC>mean+2SD of healthy) at both time-scales, and spirometry. Sensitivities were determined using ROC analysis.

Results—For asthmatics, the short- and long-time-scale group-mean ADC were 0.254±0.032 cm^2/s and 0.0237±0.0055 cm^2/s, respectively, representing a 9% and 27% (p=0.038 and p=0.005) increase compared to healthy group. The group-mean %ADC-abn were 6.4%±3.7% and 17.5% ±14.2%, representing a 107% and 272% (p=0.004 and p=0.006) increase. For COPD much greater elevations were observed. %ADC-abn provided better discrimination than mean-ADC between asthmatic and healthy subjects. In asthmatics ADC did not correlate with spirometry.

Conclusion—With long-time-scale ^{3}He diffusion magnetic resonance imaging (MRI) changes in lung microstructure were detected in asthma that were more conspicuous regionally than at the short time scale. The hybrid diffusion method is a novel means of identifying small airway disease.

Keywords

Asthma; small airways; hyperpolarized gas; hyperpolarized helium-3; MRI; diffusion MRI

INTRODUCTION

With hyperpolarized ^{3}He (H3He) diffusion Magnetic Resonance Imaging (MRI), information about the lung microstructure is obtained by measuring the degree to which diffusion-driven

*To whom correspondence should be addressed: Chengbo Wang, PhD, Department of Radiology, University of Virginia School of Medicine, Charlottesville, Virginia 22908, USA, Phone: 202-403-1875, Fax: 434-924-9435, chengbo@gmail.com.

displacement of inhaled ^{3}He atoms is restricted by the walls of the airways (1–17). Studies in animals and humans have demonstrated increases in the apparent diffusion coefficient (ADC) in subjects with chronic obstructive pulmonary disease (COPD) compared to those with healthy lungs, resulting from the enlargement of the airspaces caused by breakdown of the alveoli (1, 3,6,8,12,15,17–20). Further, regional differences in ADC values within a given subject have also been shown to correspond to differences in the degree of lung destruction (15,18). More recently, increases in ADC values have been demonstrated in healthy smokers, suggesting high sensitivity of H3He diffusion MRI for early detection of alveolar breakdown in asymptomatic individuals (6). In addition, it has been shown in children that there is a natural increase in ADC with age resulting from the normal alveolar enlargement during development (21).

There is little information on ADC changes that may occur in patients with asthma. In one study, involving 21 asthmatics, 24 healthy never smokers and 16 subjects with COPD or who were smokers, there appeared to be a slightly lower mean ADC in the asthma group compared with the healthy subjects (22). However, when corrected for age, the asthma group did not differ significantly from the healthy subjects, suggesting that the lower mean ADC in asthma was, in part, explained by their younger age. The mean ADC of the patients with COPD and the smokers was markedly elevated, as expected (22). In another study, involving only a single patient with reactive airway disease, the mean ADC was similar to that of the healthy subjects although the measured kurtosis was different (23).

H3He diffusion MRI has been used to investigate two diffusion-time regimes: the short-time scale at which H3He diffusion is observed over a few milliseconds, resulting in measured ADC values for the healthy lung in the range of 0.1 – 0.3 cm^2/s (1,3,4,16,18,20,21,24), and the long-time scale at which diffusion is observed over the period of approximately a second, yielding ADC values in the range of 0.015 – 0.045 cm^2/s for the healthy lung (25–28). The commonly used technique for measuring short-time-scale H3He diffusion has been an interleaved gradient-echo (GRE) based pulse sequence with a bipolar diffusion-sensitizing gradient (2, 18,20). Using this technique, the diffusion time corresponds to displacements of the ^{3}He atoms on the order of a few hundred micrometers, i.e., in the range of the alveolar diameter. For long-time-scale diffusion, several techniques have been developed based on the principle of storing diffusion-encoded magnetization along the longitudinal direction to substantially extend the measurable diffusion time compared to that for the GRE-based method (25–28). As noted above, the long-time-scale diffusion results in ADC values that are roughly an order of magnitude smaller than those for the short-time scale (25–28). The corresponding displacement of ^{3}He atoms is on the order of a centimeter, i.e., in the range of the acinus (29), the functional respiratory unit. Preliminary results suggest that the long-time-scale H3He diffusion method is more sensitive, permitting detection of early emphysematous changes that are not evident with the short-time-scale H3He technique (25,27). The aforementioned studies in asthma reported only short-time-scale diffusion results and, therefore, subtle differences between the asthmatics and healthy subjects could potentially have gone undetected (22,23).

The purpose of our study was to measure short- and long-time-scale diffusion of H3He in patients with asthma, and to compare the results with those from healthy volunteers and patients with COPD. To facilitate this comparison, we developed a pulse sequence that acquires co-registered ADC maps at both time scales during a single breath hold, allowing precise correlation between the H3He diffusion findings at any given anatomic level of the lung.

MATERIALS AND METHODS

ADC maps can be obtained with the established interleaved-GRE-based method for short-time-scale (diffusion time ~ 1 ms) H3He diffusion measurements while consuming only a small fraction of the H3He magnetization (2,18,20). Such a short-time-scale measurement can

therefore be appended before a stimulated-echo acquisition mode (STEAM) based long-time-scale (diffusion time ~ 1.5 s) diffusion pulse sequence (which requires a larger fraction of magnetization to yield adequate image quality) (25). Thus, by combining the two methods ADC maps with the same spatial registration corresponding to two distinct diffusion times can be acquired in a single breath-hold (30). We implemented this hybrid MRI pulse sequence using a GRE-based method identical to that used in numerous previous studies (2,18,20), and the STEAM-based method described in detail in reference (25). This hybrid pulse sequence was then used to obtain co-registered short- and long-time-scale ADC maps for this study.

To test this pulse sequence under conditions of relatively free diffusion, the pulse sequence was performed in a pillow-shaped Tedlar gas bag with dimensions 150 × 150 × 80 mm that contained 100 ml of H3He gas and 900 ml of N_2. The diffusion time was about 1 ms for the short-time scale and set to 160 ms for the long-time scale.

Healthy subjects and patients with either asthma or COPD were recruited for the study. To minimize the influence of age on the diffusion measurements, only subjects older than 40 years were included. Healthy subjects had no history or symptoms of asthma or other lung disease, no allergies, no history of smoking, and no history of routine exposure to passive smoking. The asthmatics were recruited from our institution's asthma clinics and were diagnosed by a specialist in asthma and allergy as having asthma that was considered difficult to treat. Since the goal was to image the asthmatics with as little active airway wall inflammation as possible, the patients were treated with oral corticosteroids for at least 7 days prior to being imaged. An exclusion criterion for the asthmatics was a history of smoking. Subjects with COPD had a history of smoking, a percent-predicted forced expiratory volume in one second (FEV_1% predict) less than 80%, and no other known lung diseases.

All experiments were performed under a physician's Investigational New Drug application (IND 57,866) for imaging with H3He using a protocol approved by our institutional review board. All subjects gave written informed consent prior to participation in the study. Throughout each study, the subject's heart rate and oxygen saturation level were monitored (Omni-Track Vital Signs Monitoring System, model 3100; Invivo Research Inc., Orlando FL); all studies were supervised by a radiologist.

Spirometry was performed in a seated position in each subject immediately prior to imaging using a model PB100 spirometer (Puritan Bennett; Lenexa, KS) and the Knudson 1983 reference tables for predicted normal limits (31). The FEV_1%predict and the forced vital capacity (FVC) were recorded; FEV_1%predict > 80% and FEV_1/FVC > 70 were considered normal.

^{3}He gas was polarized by collisional spin exchange with an optically pumped rubidium vapor using a prototype commercial system (Model 9600 Helium Polarizer; Magnetic Imaging Technologies Inc., Durham, NC) (32). The polarization was typically between 30% and 40%. Immediately prior to imaging, the desired volume of H3He gas (~ 400– 700 ml) was dispensed into a Tedlar bag (Jensen Inert Products, Coral Springs, FL) and diluted with medical grade N_2 to a total volume that equaled, in all but 3 healthy subjects, roughly one-third of the subject's FVC as measured by spirometry on the day of imaging. In the 3 healthy subjects, H3He was diluted with N_2 to a total volume of 1 L without consideration of FVC.

Imaging was performed using a commercial 1.5-T whole-body MR scanner (Magnetom Sonata; Siemens Medical Solutions, Malvern, PA), modified to operate at the ^{3}He resonant frequency, and a vest-shaped ^{3}He chest coil (Clinical MR Solutions, Brookfield, WI). With the subject supine in the MR scanner, breath-hold proton images of the chest were obtained for positioning the H3He images. Subsequently, the bag containing the H3He/N_2 mixture was transported to the scanner and inhaled by the subject and, using the hybrid MRI pulse sequence

a set of short- and long-time-scale axial diffusion-weighted images covering the entire lung was obtained during a breath-hold period lasting no more than 15 s. The total time for this procedure, including positioning of the subject in the chest coil on the MR-scanner table, acquiring scout proton images, and acquiring H3He images, was typically less than 20 min.

The pulse-sequence parameters for the short-time-scale ADC measurement included: TR, 7.5 ms; TE, 4.8 ms; flip angle, 1.7°; *b* values, 0 and 1.6 s/cm^2. The pulse-sequence parameters for the long-time-scale ADC measurement included: TR, 6.4 ms; TE_1, 1.3 ms; flip angle, 5°; TE_2, 7 ms; TM, 1.39 s; δ, 0.15 ms; Δ, 1.385 s; diffusion time, 1.5 s; *b* value, 60 s/cm^2. Other parameters of the hybrid pulse sequence included: field-of-view, 300 – 350 × 350 – 400 mm^2; matrix, 48 – 60 × 64; slice thickness, 30 – 40 mm; interslice gap, 0 – 20%.

The raw (untransformed) measurement data were transferred from the scanner to a personal computer for post-processing. All analyses were performed using our custom routines programmed in MATLAB (The Mathworks, Natick, MA). Since the hybrid MRI pulse sequence combined the commonly used GRE-based short-time-scale diffusion sequence as described in Reference (18) and the STEAM-based long-time-scale diffusion sequence as described in Reference (25), the ADC maps were computed from diffusion-weighted images on a pixel-by-pixel basis following the respective formulas at the corresponding time scales (18,25).

The axial ADC maps were reviewed by a radiologist blinded to the demographic information and disease status. The reviewer scored the ADC maps at the short- and long-time scales independently without knowledge of the time scale. For each time scale and each subject, the ADC maps were scored as homogeneous, mildly (<15% of lung area with focally elevated ADC), moderately (15–50% of lung area with elevated ADC) or severely heterogeneous (>50% of lung area with elevated ADC), and the regional distribution of elevated ADC values were scored as upper lobe predominant, lower lobe predominant, or mixed.

The mean signal-to-noise ratio (SNR) of the *b*=0 image, and mean and standard deviation (SD) of the ADC values were calculated for both time scales in each subject. Since there is, to our knowledge, no standard, generally-accepted upper limit for ADC values in healthy subjects we used, as an upper-limit threshold for the normal ADC value for each of the two time scales, the value that was two standard deviations (SDs) above the mean based on the ADC values from all pixels for all healthy subjects (33). The percentage of pixels whose ADC value was greater than the respective threshold was then calculated for each subject and each time scale, and termed %ADC-abn where abn stands for abnormal. After the SNR, ADC and %ADC-abn values were calculated for each subject, the mean, SD and coefficient of variation of these three parameters for each time scale were calculated for the three groups (healthy, asthma and COPD). A pairwise comparison of the group mean values of ADC and %ADC-abn was performed using an unpaired two tailed *t*-test. The relationship between the ADC and spirometry parameters was analyzed with linear regression in each of the three groups. The performances of the various parameters in discriminating asthma or COPD from healthy subjects were studied by using non-parametric receiver operating characteristic (ROC) curves (34), and areas under the ROC curves were determined.

RESULTS

For the ADC map from the Tedlar gas-bag phantom, the mean ADC was 0.86 ± 0.01 cm^2/s (mean ± SD) at a diffusion time of 1 ms, which is within the range of values reported for the free diffusion coefficient of dilute ^{3}He in air or N_2 (reported normal range: 0.83 – 0.88 cm^2/s) (20,27,35). The mean ADC was 0.80 ± 0.11 cm^2/s at a diffusion time of 160 ms.

Fourteen clinically healthy subjects (6 males, 8 females; age: 54.9 ± 6.3 yrs), 14 patients with asthma (8 males, 6 females; age: 56.6 ± 11.2 yrs) and 9 subjects with smoking-related COPD (5 males, 4 females; age: 64.9 ± 4.8 yrs) were enrolled in the study, Table 1. All subjects were able to inhale the H3He/N_2 gas, perform the required breath-hold maneuvers and tolerate the MR scan without difficulty. Co-registered ADC maps at both short- and long-time scales were obtained in all subjects. Among the three groups of subjects, there were no significant differences in gender, height, or weight. The asthma and healthy groups were similar in age; the COPD group was slightly older than other two groups, $p<0.026$, Table 1.

Twelve (86%) of the 14 healthy subjects had a homogeneous appearance of short-time-scale ADC maps, while only 4 (29%) of 14 had homogeneous long-time-scale ADC maps, $p=0.006$. However, of those that had heterogeneous ADC maps at the long-time scale, 9 (90%) of 10 were mildly heterogeneous, and 5 (50%) of 10 had upper lobe predominance of elevated ADC values. Representative ADC maps from a healthy subject at both short- and long-time scale are shown in Figs. 1a and 1b, respectively, showing homogenously low ADC values. As shown in Table 1, the group-mean ADC for healthy subjects was 0.234 ± 0.020 cm^2/s for the short-time scale and 0.0186 ± 0.0026 cm^2/s for the long-time scale, almost a factor of 13 difference. The upper-limit threshold for normal ADC values, determined as that value which was two SDs above the mean of the set of all ADC values from all healthy subjects, was 0.35 cm^2/s for the short-time scale and 0.034 cm^2/s for the long-time scale. In concordance with the visual scoring, only a small percent of the ADC values exceeded these thresholds in the majority of healthy subjects. At the short-time scale the %ADC-abn for all healthy subjects was ≤ 6%, and for the long-time scale it was ≤ 5% in 12 (86%) of 14 subjects and 22% and 12%, respectively, in the remaining two. For the short-time scale both the mean ADC and the %ADC-abn were concentrated in a very narrow range, Fig. 2a and Fig. 3a. For the long-time scale the larger ranges were predominantly determined by the two aforementioned outliers, Fig. 2b and Fig. 3b. All healthy subjects had FEV_1%predict and FEV_1/FVC values within the clinically accepted normal range. There was no correlation between mean ADC or %ADC-abn at either time scale and FEV_1%predict or FEV_1/FVC in the healthy group ($|r|<0.43$; $p>0.120$).

In the group of patients with asthma there were 10 (71%) of 14 who had a mildly heterogeneous appearance of short-time-scale ADC maps. At the long-time scale, 12 (86%) of 14 had a heterogeneous appearance, with 9 of these being mild, 2 moderate, and 1 severe. Co-registered ADC maps for a representative asthmatic subject with focal elevations in the ADC maps are presented in Figs. 1c and 1d, showing greater conspicuity of the findings at the long-time scale. The group-mean ADC of the asthmatics was elevated relative to that for the healthy group for both time scales (short-time scale, 0.254 ± 0.032 cm^2/s, an increase of 9% compared to healthy group, $p=0.038$; long-time scale, 0.0237 ± 0.0055 cm^2/s, an increase of 27%, $p=0.005$), Figs. 2a and 2b. The group-mean %ADC-abn for patients with asthma was also elevated relative to the healthy subjects (short-time scale, 6.4% ± 3.7%, an increase of 107% compared with the healthy subjects, $p=0.004$; long-time scale, 17.5% ± 14.2%, an increase of 272%, $p=0.006$), Figs. 3a and 3b. There was no correlation between mean ADC or %ADC-abn and FEV_1% predict or FEV_1/FVC in the asthmatic group ($|r|<0.29$; $p>0.350$) for either time scale. The areas under ROC curve were 0.72 and 0.82 for the mean ADC, and were 0.83 and 0.85 for %ADC-abn for the short- and long-time-scale, respectively, Figs. 4a and 4b.

For the group with COPD, the ADC maps for both time scales were severely heterogeneous in 6 (67%) of 9 subjects; in the remaining three heterogeneity was either mild or moderate. Co-registered ADC maps at the two time scales from a representative subject with COPD (FEV_1%predict: 69%) showing severely elevated ADC values are presented in Figs. 1e and 1f. For the COPD subjects, the group-mean ADC was 0.404 ± 0.113 cm^2/s for the short-time scale, and 0.0404 ± 0.0077 cm^2/s for the long-time scale. As expected, these values were significantly greater relative to the healthy subjects (short-time scale, 71% elevation, $p=0.002$;

long-time scale, 117% elevation, $p<0.001$), Figs. 2a and 2b. The group-mean %ADC-abn for subjects with COPD was markedly elevated relative to that for the healthy subjects (short-time scale, 53.7% ± 29.4%, $p<0.001$; long-time scale, 66.6% ± 23.1%, $p<0.001$), Figs. 3a and 3b. These values were also significantly greater than those for patients with asthma, $p<0.005$, Fig. 2 and Fig. 3. There was a strong negative correlation between short-time-scale mean ADC and FEV_1%predict or FEV_1/FVC in the COPD subjects ($r<-0.8$; $p<0.010$), also a strong negative correlation between short-time-scale %ADC-abn and FEV_1/FVC ($r=-0.82$; $p=0.008$), while only a moderate negative correlation appeared between short-time-scale %ADC-abn and FEV_1%predict ($r=-0.60$; $p=0.089$); however, no correlation was observed between long-time-scale mean ADC or %ADC-abn and spirometry parameters ($|r|<0.38$; $p>0.314$). The areas under the ROC curves comparing COPD with healthy subjects were 1.00 for both the mean ADC and the %ADC-abn for both time scales.

The mean ADC and %ADC-abn values of the short- and the long-time scale for each subject are plotted in Figs. 5a and 5b. There was a moderate correlation between the short- and long-time-scale mean ADC in the asthmatic group ($r=0.57$, $p=0.033$) which was not present in the healthy group ($r=0.05$, $p=0.847$) or the COPD group ($r=0.31$, $p=0.426$), Fig. 5a. Similarly for %ADC-abn, there was a stronger, but still moderate, correlation for asthmatics ($r=0.67$, $p=0.009$), but not for the healthy group ($r=0.18$, $p=0.548$) or the COPD group ($r=0.22$, $p=0.570$), Fig. 5b.

DISCUSSION

The main advantage of the hybrid MRI pulse sequence that we developed is that the short- and long-time-scale ADC maps are generated from the exact same anatomic level because the data for the two time scales are obtained during the same, single breath hold. As a result, pixel-by-pixel comparisons can be accurately performed and differences in ^{3}He displacement can be determined without the interference of artifacts from misregistration. Considering that H3He diffusion measurements at different time scales are thought to probe different anatomic length scales, it would seem that alterations in the lung microstructure can be more readily detected using this pulse sequence. We found in the patients with asthma that both short- and long-time-scale ADC values were increased significantly compared with those of healthy subjects. In the COPD patients these values were even more elevated, as would be expected from the enlargement of the airspaces that typically occurs in this disease (36). However, the cause of the ADC elevation in the lungs of the patients with asthma is less certain as breakdown of the alveoli is not an expected feature in this disease (37). Nevertheless, focal hyperlucencies on CT are commonly found in asthmatics and are frequently ascribed to regional “air-trapping”, a process whereby there is abnormal regional retention of air in the lungs after expiration (38). Air enters the terminal bronchi and alveoli on inspiration but closure of the bronchi on expiration “traps” the air. This is occurring in the small airways and is not ideally detected by the FEV_1, the test that reflects the function of both large and small airways (39). It seems plausible that these regions of air-trapping would lead to focal elevation in ADC values. Alternatively, emphysema, including subclinical emphysema, can cause elevations in ADC (6). However, since emphysema is uncommon in asthmatics, as was shown in autopsy studies (37), it seems more likely that air-trapping was a dominant factor causing the ADC elevations in the asthmatic subjects in this study. As seen in prior studies (1,3,6,8,[12],17,18,27,28), we found that the subjects with COPD had markedly elevated ADC values over large regions, which previously has been assumed to be secondary to emphysematous changes within the lung. However, our results in the asthmatics suggest that the ADC elevations in patients with COPD may be caused by a combination of emphysematous tissue destruction and regional lung hyperexpansion, both processes known to occur in patients with COPD (36).

Asthma is a chronic inflammatory, respiratory disease that affects predominantly either the small or large airways, or sometimes both. The inflammation that is present in the airway walls makes the airways sensitive to irritants; however, the microstructural changes in lung tissue of subjects with asthma are not well understood. The ADC maps from most of the subjects with asthma were heterogeneous with focal elevations, suggesting that microstructural changes within the lung are heterogeneous. Although the exact cause of these ADC elevations is not yet known, they likely represent important changes of the lung microstructure. The regional distribution of these changes lends insight into the underlying pathophysiology of asthma and the related abnormalities of the lung microstructure. This has important implications. Since patients with small airway disease may have different disease processes than those with large airway disease, it may be that the disease has different phenotypes (40,41). Further, as small airway disease is not well reflected in the usual spirometric measures used to monitor asthma, patients can have severe disease that could thereby be missed by spirometry (39). Also, there are therapeutic implications with respect to inhalant drugs that are normally used to treat asthma as these may not necessarily access the small airways.

As noted above, measurement of H3He diffusion at two time scales during a single breath hold is thought to provide information about the lung microstructure on two anatomic levels. The length scale corresponding to short-time-scale ADC values is such that these measurements are thought to primarily be sensitive to changes at the alveolar level (16,18). Because long-time-scale ADC values correspond to longer length scales, such measurements may be sensitive to factors that affect the connectivity of the small airways (25,27,28). From our results it appears that, on a regional basis, the changes in the long-time-scale ADC are more extensive and more severe than those in the short-time-scale ADC. This increase in regional sensitivity did not translate into much improvement in the discrimination between healthy subjects and asthmatics, at least with the summary ADC metrics used in this study. However, the apparently increased sensitivity of the long-time-scale ADC to regional changes in the lung may be of importance in understanding asthma and assessing the response to treatment.

Most asthmatics had only small, focally elevated areas on their ADC maps, and such small regions of elevation had little effect on the mean ADC. However a metric such as %ADC-abn is designed to be sensitive to small areas of ADC elevation, and thus, it is not surprising that this parameter provided better discrimination between the healthy subjects and asthmatics than mean ADC. The subjects with COPD had such marked and extensive elevations in ADC that all of the ADC metrics we evaluated perfectly discriminated between the healthy subjects and the subjects with COPD.

The ADC values for healthy subjects were clustered in a very small range which may have resulted in the lack of correlation between the long- and short-time-scale ADC in this group, as shown in Figs. 5a and 5b. For the subjects with COPD the lack of correlation may have been due to a relative clustering of the long-time-scale ADC values toward the top of the scale. Thus, the increased regional sensitivity of the long-time-scale ADC is useful in detecting mild or early disease. However, in patients with severe disease, the ability to distinguish relative disease severity may be lost which is confirmed by the stronger correlation of the short-time-scale ADC than the long-time-scale ADC with spirometry in the COPD patients. Interestingly, in the asthmatics, there was a moderate correlation between the short- and long-time-scale ADC, suggesting that, whatever process is causing the elevations at one time (length) scale, it is likely affecting the other time (length) scale as well. However, in the asthma group, we did not find an association between the ADC metrics and spirometry. Thus, the imaging may provide new information about the changes in the lung microstructure in asthma that may not be obtainable by other means. Of course, the patient's position may have played a role since imaging was done in supine position while spirometry was measured with the patients sitting upright.

Our results in the healthy subjects and patients with COPD agree well with the results from many prior studies, that is, there were large differences in ADC values between groups at both time scales (3,6,8,16–18,20,27,28). In our study we also found significant differences in ADC values between asthmatic and healthy subjects. No such differences were found by others (22,23). However, in one of those studies involving 21 patients with asthma, the asthmatic patients were generally younger in age and had higher FEV_1 values compared to our patients (22). Also only the asthmatic patients who were difficult to treat were included in our study. Another study involved only one subject with reactive airway dysfunction syndrome, an asthma-like syndrome that occurs in nonallergic individuals in response to an inhalational injury (23). Since our patients with asthma all had oral corticosteroids before imaging to suppress active inflammation, it is likely that the changes in diffusion we observed do not represent acute inflammation or bronchospasm but might reflect tissue remodeling including permanent changes in airway structure.

A disadvantage of the hybrid pulse sequence is that a longer breath hold time is required to acquire the data than when a single diffusion technique was used. However, the extended breath hold period used in this study was tolerated by all subjects without difficulty. Furthermore, the registration of ADC maps at the two time scales is sensitive to patient motion during the acquisition. Another drawback of the long-time scale method with the parameters used in this study is that, in case of very large ADC values, the diffusion-weighted signal is quickly driven below the noise level (25). As a result, in subjects such as patients with COPD who have extremely elevated ADC values, these long-time scale ADC values cannot be determined accurately, and this may have affected the results in the COPD group.

In conclusion, we used a novel hybrid MR pulse sequence to obtain co-registered ADC maps at both short- and long-time scales during a single breath hold, and demonstrated significant elevations in ADC values in patients with asthma compared to healthy subjects, and, as expected, even more markedly elevations in the patients with COPD. On the long-time scale ADC maps the elevations in the asthma group were heterogeneous and substantially larger than on the short-time scale images, and involved, in most cases, greater areas of the lung. The cause of the elevations in asthma is uncertain but possibly, the changes reflect tissue remodeling including permanent changes in airway structure. Further studies will be needed to determine the nature of these abnormalities. The hybrid diffusion MR pulse sequence might provide a novel means of identifying small airway disease.

Acknowledgments

Grant Support:

Supported by grants R01-HL066479 and R01-HL079077 from the National Heart, Lung, and Blood Institute, a Clinical Innovator Award from the Flight Attendant Medical Research Institute and Siemens Medical Solutions. The content is solely the responsibility of the authors and does not necessarily represent the official views of the National Heart, Lung, and Blood Institute or the National Institutes of Health.

The authors thank John M. Christopher, RT(R)(MR), Doris A. Harding, RN and Joanne C. Gersbach, RN for valuable assistance with the MR experiments and scheduling of subjects, Dr. Jing Cai for his expert operation of the helium polarization system, and Dr. Abbas F. Jawad for his help on ROC analysis.

REFERENCES

1. Bink A, Hanisch G, Karg A, et al. Clinical aspects of the apparent diffusion coefficient in (3)He MRI: Results in healthy volunteers and patients after lung transplantation. J Magn Reson Imaging 2007;25 (6):1152–1158. [PubMed: 17520719]
2. Bock M. Simultaneous T2* and diffusion measurements with 3He. Magn Reson Med 1997;38(6):890–895. [PubMed: 9402189]

3. Chen XJ, Hedlund LW, Moller HE, Chawla MS, Maronpot RR, Johnson GA. Detection of emphysema in rat lungs by using magnetic resonance measurements of 3He diffusion. Proc Natl Acad Sci U S A 2000;97(21):11478–11481. [PubMed: 11027348]
4. Conradi MS, Yablonskiy DA, Woods JC, et al. 3He diffusion MRI of the lung. Acad Radiol 2005;12 (11):1406–1413. [PubMed: 16253852]
5. Dimitrov IE, Charagundla SR, Rizi R, Reddy R, Leigh JS. An MR imaging method for simultaneous measurement of gaseous diffusion constant and longitudinal relaxation time. Magn Reson Imaging 1999;17(2):267–273. [PubMed: 10215482]
6. Fain SB, Panth SR, Evans MD, et al. Early emphysematous changes in asymptomatic smokers: detection with 3He MR imaging. Radiology 2006;239(3):875–883. [PubMed: 16714465]
7. Ishii M, Fischer MC, Emami K, et al. Hyperpolarized helium-3 MR imaging of pulmonary function. Radiol Clin North Am 2005;43(1):235–246. [PubMed: 15693659]
8. Ley S, Zaporozhan J, Morbach A, et al. Functional evaluation of emphysema using diffusion-weighted 3Helium-magnetic resonance imaging, high-resolution computed tomography, and lung function tests. Invest Radiol 2004;39(7):427–434. [PubMed: 15194914]
9. Mayo JR, Hayden ME. Hyperpolarized helium 3 diffusion imaging of the lung. Radiology 2002;222 (1):8–11. [PubMed: 11756698]
10. Morbach AE, Gast KK, Schmiedeskamp J, et al. Diffusion-weighted MRI of the lung with hyperpolarized helium-3: a study of reproducibility. J Magn Reson Imaging 2005;21(6):765–774. [PubMed: 15906344]
11. Parraga G, Ouriadov A, Evans A, et al. Hyperpolarized 3He ventilation defects and apparent diffusion coefficients in chronic obstructive pulmonary disease: preliminary results at 3.0 Tesla. Invest Radiol 2007;42(6):384–391. [PubMed: 17507809]
12. Swift AJ, Wild JM, Fichele S, et al. Emphysematous changes and normal variation in smokers and COPD patients using diffusion 3He MRI. Eur J Radiol 2005;54(3):352–358. [PubMed: 15899335]
13. van Beek EJ, Wild JM, Kauczor HU, Schreiber W, Mugler JP 3rd, de Lange EE. Functional MRI of the lung using hyperpolarized 3-helium gas. J Magn Reson Imaging 2004;20(4):540–554. [PubMed: 15390146]
14. Wild JM, Woodhouse N, Teh K. Single-scan acquisition of registered hyperpolarized (3)He ventilation and ADC images using a hybrid 2D gradient-echo sequence. Magn Reson Med 2007;57 (6):1185–1189. [PubMed: 17534918]
15. Woods JC, Choong CK, Yablonskiy DA, et al. Hyperpolarized 3He diffusion MRI and histology in pulmonary emphysema. Magn Reson Med 2006;56(6):1293–1300. [PubMed: 17058206]
16. Yablonskiy DA, Sukstanskii AL, Leawoods JC, et al. Quantitative in vivo assessment of lung microstructure at the alveolar level with hyperpolarized 3He diffusion MRI. Proc Natl Acad Sci U S A 2002;99(5):3111–3116. [PubMed: 11867733]
17. Peces-Barba G, Ruiz-Cabello J, Cremillieux Y, et al. Helium-3 MRI diffusion coefficient: correlation to morphometry in a model of mild emphysema. Eur Respir J 2003;22(1):14–19. [PubMed: 12882445]
18. Salerno M, de Lange EE, Altes TA, Truwit JD, Brookeman JR, Mugler JP 3rd. Emphysema: hyperpolarized helium 3 diffusion MR imaging of the lungs compared with spirometric indexes--initial experience. Radiology 2002;222(1):252–260. [PubMed: 11756734]
19. Tanoli TS, Woods JC, Conradi MS, et al. In vivo lung morphometry with hyperpolarized 3He diffusion MRI in canines with induced emphysema: disease progression and comparison with computed tomography. J Appl Physiol 2007;102(1):477–484. [PubMed: 16873601]
20. Saam BT, Yablonskiy DA, Kodibagkar VD, et al. MR imaging of diffusion of (3)He gas in healthy and diseased lungs. Magn Reson Med 2000;44(2):174–179. [PubMed: 10918314]
21. Altes TA, Mata J, de Lange EE, Brookeman JR, Mugler JP 3rd. Assessment of lung development using hyperpolarized helium-3 diffusion MR imaging. J Magn Reson Imaging 2006;24(6):1277–1283. [PubMed: 17096396]
22. Fain SB, Altes TA, O'Halloran R, et al. Comparison of diffusion weighted helium-3 MRI in patients with asthma versus those with COPD. 2006 May, 6–12; Seattle, WA, USA. Proc. Intl. Soc. Mag. Reson. Med 15:1665.

23. Trampel R, Jensen JH, Lee RF, Kamenetskiy I, McGuinness G, Johnson G. Diffusional kurtosis imaging in the lung using hyperpolarized 3He. Magn Reson Med 2006;56(4):733–737. [PubMed: 16958076]
24. Fain SB, Altes TA, Panth SR, et al. Detection of age-dependent changes in healthy adult lungs with diffusion-weighted 3He MRI. Acad Radiol 2005;12(11):1385–1393. [PubMed: 16253850]
25. Wang C, Miller GW, Altes TA, de Lange EE, Cates GD Jr, Mugler JP 3rd. Time dependence of 3He diffusion in the human lung: measurement in the long-time regime using stimulated echoes. Magn Reson Med 2006;56(2):296–309. [PubMed: 16791861]
26. Fichele S, Paley MN, Woodhouse N, Griffiths PD, van Beek EJ, Wild JM. Measurements and modeling of long range 3He diffusion in the lung using a "slice-washout" method. J Magn Reson 2005;174(1):28–33. [PubMed: 15809169]
27. Woods JC, Yablonskiy DA, Chino K, Tanoli TS, Cooper JD, Conradi MS. Magnetization tagging decay to measure long-range (3)He diffusion in healthy and emphysematous canine lungs. Magn Reson Med 2004;51(5):1002–1008. [PubMed: 15122683]
28. Woods JC, Yablonskiy DA, Choong CK, et al. Long-range diffusion of hyperpolarized 3He in explanted normal and emphysematous human lungs via magnetization tagging. J Appl Physiol 2005;99(5):1992–1997. [PubMed: 16024528]
29. Schreider JP, Raabe OG. Structure of the human respiratory acinus. Am J Anat 1981;162(3):221–232. [PubMed: 7315750]
30. Wang C, Miller GW, Altes TA, et al. Measurement of the Diffusion of Hyperpolarized 3He in Human Lungs over Short and Long Time Scales During One Breath Hold. 2007; Berlin, Germany. Proc. Intl. Soc. Mag. Reson. Med 16:1284.
31. Knudson RJ, Lebowitz MD, Holberg CJ, Burrows B. Changes in the normal maximal expiratory flow-volume curve with growth and aging. Am Rev Respir Dis 1983;127(6):725–734. [PubMed: 6859656]
32. Happer W, Miron E, Schaefer S, Schreiber D, van-Wijingaarden WA, Zeng X. Polarization of the nuclear spins of noble-gas atoms by spin exchange with optically pumped alkali-metal atoms. Phys Rev A 1984;29:3092–3110.
33. de Lange EE, Altes TA, Patrie JT, et al. Evaluation of Asthma With Hyperpolarized Helium-3 MRI: Correlation With Clinical Severity and Spirometry. Chest 2006;130(4):1055–1062. [PubMed: 17035438]
34. Obuchowski NA. Receiver Operating Characteristic Curves and Their Use in Radiology. Radiology 2003;229(1):3–8. [PubMed: 14519861]
35. Chen XJ, Moller HE, Chawla MS, et al. Spatially resolved measurements of hyperpolarized gas properties in the lung in vivo. Part I: diffusion coefficient. Magn Reson Med 1999;42(4):721–728. [PubMed: 10502761]
36. Barnes PJ, Stockley RA. COPD: current therapeutic interventions and future approaches. Eur Respir J 2005;25(6):1084–1106. [PubMed: 15929966]
37. Leslie, KO.; Wick, MR. Practical Pulmonary Pathology: A Diagnostic Approach (Hardcover). Philadelphia, PA: Churchill Livingstone; 2004.
38. Arakawa H, Webb WR. Air trapping on expiratory high-resolution CT scans in the absence of inspiratory scan abnormalities: correlation with pulmonary function tests and differential diagnosis. AJR Am J Roentgenol 1998;170(5):1349–1353. [PubMed: 9574614]
39. Kraft M, Djukanovic R, Wilson SJ, Holgate ST, Martin RJ. Alveolar tissue inflammation in asthma. Am J Resp Crit Care Med 1996;154(5):1505–1510. [PubMed: 8912772]
40. Chanez P, Wenzel SE, Anderson GP, et al. Severe asthma in adults: What are the important questions? J Allergy Clin Immunol 2007;119(6):1337–1348. [PubMed: 17416409]
41. Moore WC, Bleecker ER, Curran-Everett D, et al. Characterization of the severe asthma phenotype by the National Heart, Lung, and Blood Institute's Severe Asthma Research Program. J Allergy Clin Immunol 2007;119(2):405–413. [PubMed: 17291857]

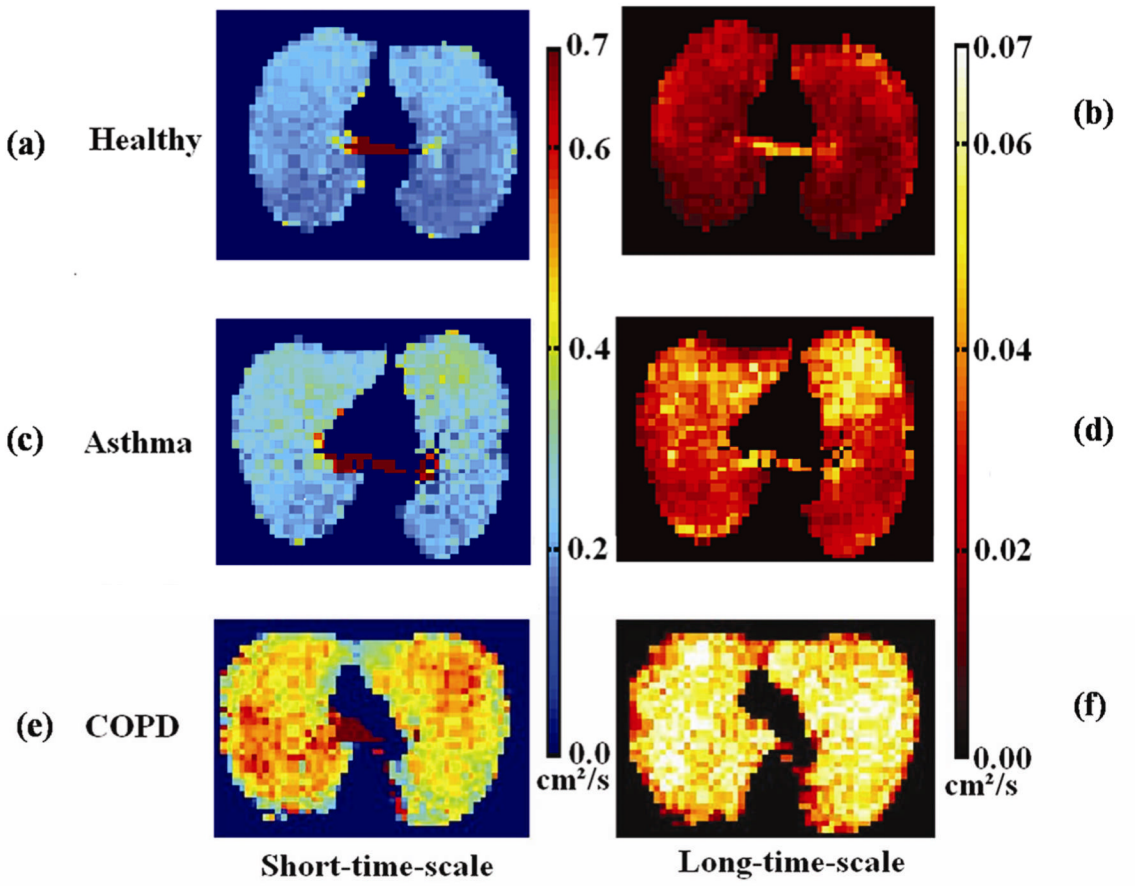

Figure 1.

Co-registered axial ADC maps from: healthy subject #7 at diffusion times of (a) 1 ms and (b) 1.5 s; asthma subject # 6 at diffusion times of (c) 1 ms and (d) 1.5 s; and COPD subject #1 at diffusion times of (e) 1 ms and (f) 1.5 s. The healthy subject has homogeneously low ADC values at both time scales. The asthmatic has focal areas of elevated ADC values anteriorly that are larger and more conspicuous on the long-time-scale ADC maps. The subject with COPD has diffusely, markedly elevated ADC values.

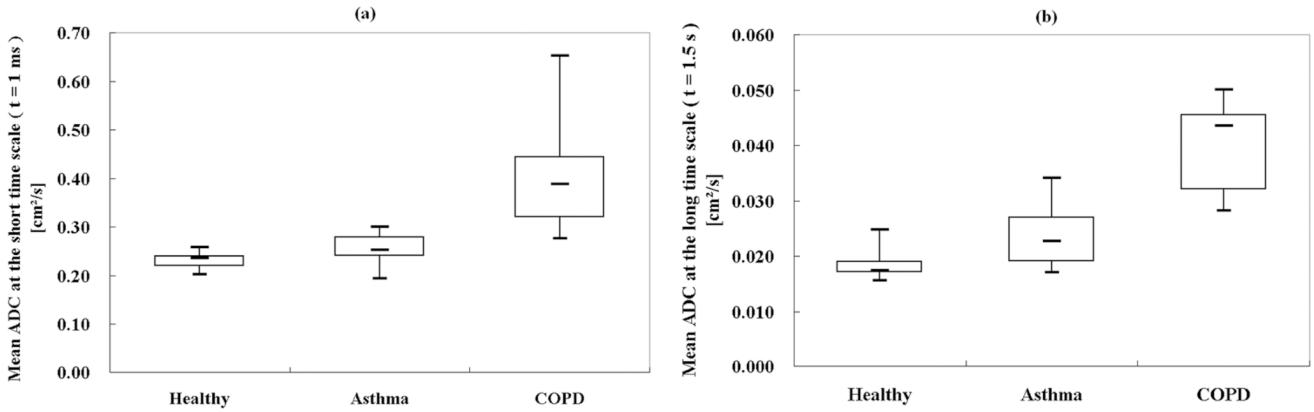

Figure 2.

Box plot of mean ADC values from each subject group for (a) the short-time scale (t = 1 ms) and (b) the long-time scale (t = 1.5 s). All mean ADC values of the healthy subjects are concentrated in a narrow range. The asthmatics have mildly elevated mean ADC values, and the subjects with COPD have markedly elevated mean ADC values. The three groups are better separated on the long-time-scale ADC (Short-time-scale: $P_{\text{asthma-healthy}} = 0.038$; $P_{\text{COPD-healthy}} = 0.002$; $P_{\text{COPD-asthma}} = 0.005$. Long-time-scale: $P_{\text{asthma-healthy}} = 0.005$; $P_{\text{COPD-healthy}} < 0.001$; $P_{\text{COPD-asthma}} = 0.005$.). Each box extends from the 25th percentile at lower edge to the 75th percentile at upper edge; the median is shown as a short line within the box. The upper and lower lines outside of the boxes represent the extreme values.

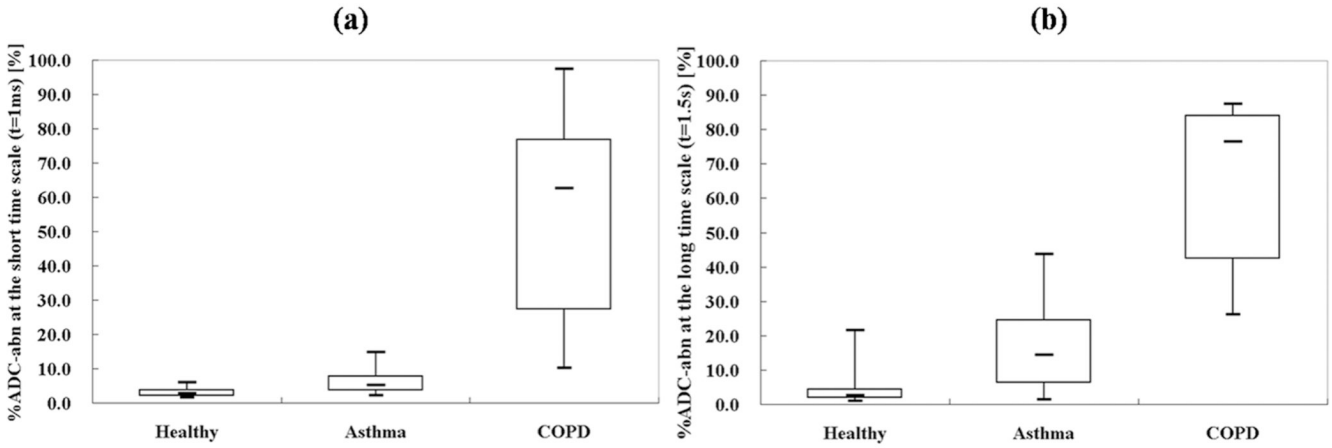

Figure 3.

Box plot of %ADC-abn values from each subject group for (a) the short-time scale (t = 1 ms) and (b) the long-time scale (t = 1.5 s). The three groups are better separated on the long-time-scale %ADC-abn (Short-time-scale: $P_{\text{asthma-healthy}} = 0.004$; $P_{\text{COPD-healthy}} < 0.001$; $P_{\text{COPD-asthma}} = 0.001$. Long-time-scale: $P_{\text{asthma-healthy}} = 0.006$; $P_{\text{COPD-healthy}} < 0.001$; $P_{\text{COPD-asthma}} < 0.001$.). The figure notation is the same as in Fig. 2.

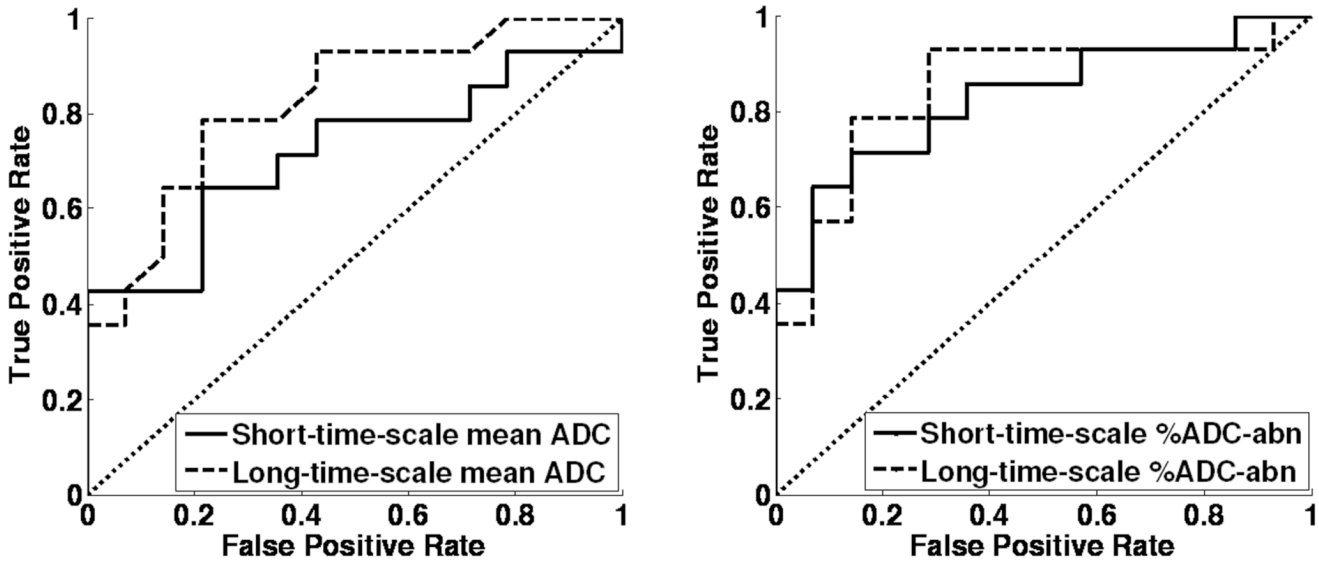

Figure 4.

ROC curves of healthy subjects and asthmatics at both time scales for (a) the mean ADC; and (b) the %ADC-abn. The long-time-scale mean ADC has a larger area under the ROC curve than the short-time-scale mean ADC indicating that it provides better discrimination between the asthmatic and healthy subjects. Further, the %ADC-abn provides better discrimination between the asthmatic and healthy subjects than the mean ADC at both time scales. (The areas under the ROC curves were 0.72 for the short-time-scale mean ADC, 0.82 for the long-time-scale mean ADC, and were 0.83 and 0.85 for the short- and long-time-scale %ADC-abn, respectively.)

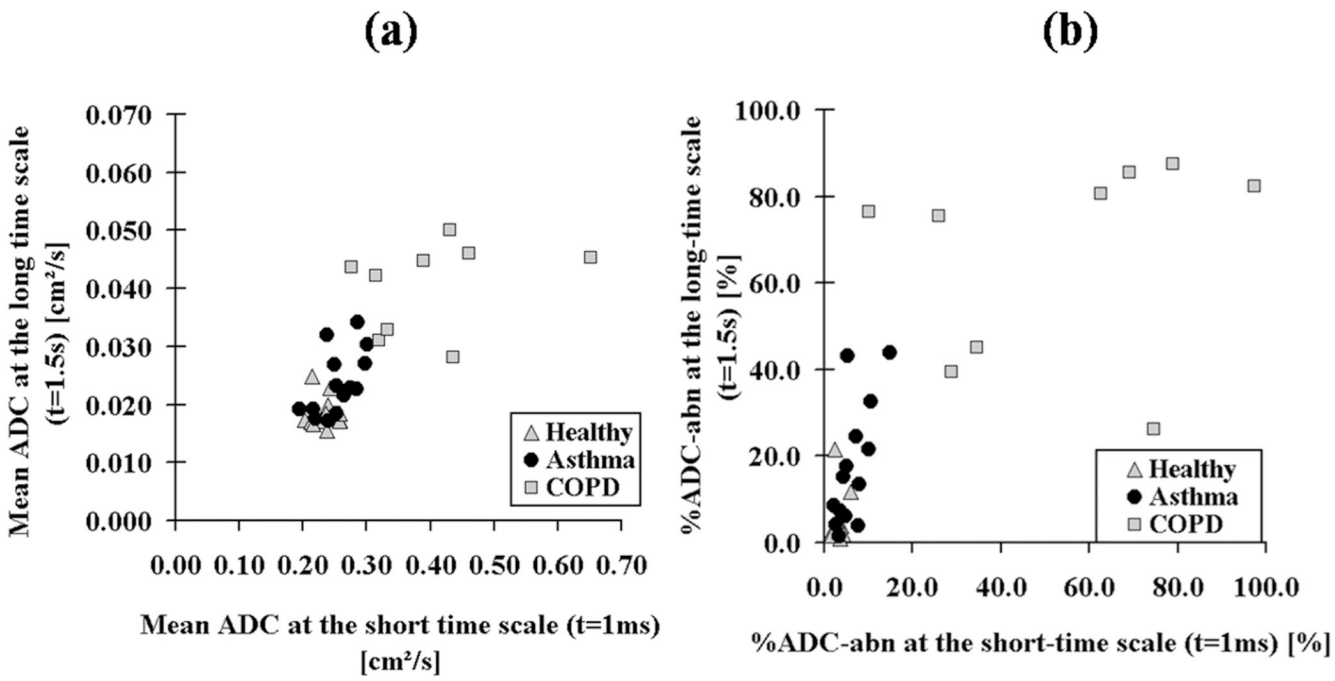

Figure 5.

Scatter plots for all subjects between both time scales showing (a) the mean ADC values; and (b) the %ADC-abn values. The healthy subjects are clustered with small mean ADC and % ADC-abn values at both time scales. The majority of COPD subjects have markedly elevated mean ADC and %ADC-abn values at both time scales. The asthmatics have a moderate correlation between mean ADC (r=0.57, p=0.033) at the two time scales; similarly for %ADC-abn, there was a stronger, but still moderate correlation (r=0.67, p=0.009).

Table 1

Demographic information, spirometry and summary of ADC results for all subjects.

Subject Number	Age (yrs)	Gender	FEV_1 %Pred (%)	Short-time-scale ADC at t = 1 ms			Long-time-scale ADC at t = 1.5 s		
				SNR[1]	Mean ADC (cm^2/s)	%ADC -abn	SNR[2]	Mean ADC (cm^2/s)	%ADC -abn
Healthy									
1	58	M	104	38	0.24	4	73	0.019	4
2	58	M	107	40	0.24	3	71	0.020	4
3	53	F	112	74	0.23	2	142	0.018	3
4	66	F	105	51	0.24	2	100	0.018	3
5	59	M	92	32	0.26	4	62	0.017	2
6	46	F	100	45	0.22	2	76	0.017	2
7	62	F	98	87	0.20	2	157	0.017	2
8	61	F	86	72	0.24	4	122	0.016	1
9	46	F	105	80	0.26	4	152	0.017	2
10	55	M	91	57	0.26	3	103	0.019	2
11	47	F	106	75	0.21	2	149	0.025	22
12	50	M	108	64	0.24	6	131	0.023	12
13	51	M	86	70	0.21	3	130	0.017	5
14	57	F	109	68	0.22	2	123	0.017	2
Mean	54.9	-	100.6	60.9	0.234	3.1	113.6	0.0186	4.7
(SD)	(6.3)	-	(8.7)	(17.2)	(0.020)	(1.2)	(32.8)	(0.0026)	(5.7)
CV^3 (%)	11.5	-	8.7	28.2	8.5	38.7	28.9	14.0	121.3
Asthma									
1	43	F	58	51	0.24	5	83	0.032	43
2	66	M	52	90	0.29	15	150	0.034	44
3	44	M	52	27	0.22	4	39	0.019	7
4	64	F	63	107	0.27	4	182	0.023	15
5	51	M	89	44	0.25	7	84	0.027	25
6	41	F	75	62	0.19	2	126	0.019	9

Subject Number	Age (yrs)	Gender	FEV_1 %Pred (%)	Short-time-scale ADC at t = 1 ms			Long-time-scale ADC at t = 1.5 s		
				SNR[1]	Mean ADC (cm^2/s)	%ADC -abn	SNR[2]	Mean ADC (cm^2/s)	%ADC -abn
7	65	M	32	59	0.28	8	104	0.023	14
8	74	F	69	49	0.26	5	80	0.022	6
9	53	F	78	56	0.25	5	99	0.023	18
10	67	M	75	69	0.30	11	124	0.030	33
11	50	M	64	28	0.25	8	58	0.018	4
12	62	M	102	34	0.24	3	65	0.017	1
13	69	M	98	60	0.30	10	120	0.027	22
14	44	F	54	68	0.22	3	130	0.018	4
Mean	56.6	-	68.6	57.4	0.254	6.4	103.1	0.0237	17.5
(SD)	(11.2)	-	(19.3)	(22.2)	(0.032)	(3.7)	(38.5)	(0.0055)	(14.2)
CV[3] (%)	19.8	-	28.1	38.7	12.6	57.8	37.3	23.2	81.4
Inc[4] (%)	3.1	-	−31.8	−3.5	8.6	106.5	−9.2	27.4	272.3
COPD									
1	61	F	69	54	0.39	63	95	0.045	81
2	71	M	58	32	0.32	29	49	0.031	40
3	62	M	64	61	0.46	69	94	0.046	86
4	62	M	71	65	0.31	26	108	0.042	75
5	73	F	69	66	0.43	79	118	0.050	88
6	61	M	64	39	0.33	35	69	0.033	45
7	61	F	27	54	0.65	97	99	0.045	82
8	69	M	49	90	0.44	75	136	0.028	26
9	64	F	68	69	0.28	10	123	0.044	76
Mean	64.9	-	59.9	58.9	0.401	53.7	99.0	0.0404	66.6
(SD)	(4.8)	-	(14.1)	(14.1)	(0.113)	(29.4)	(27.0)	(0.0077)	(23.1)
CV[3] (%)	7.4	-	23.5	23.9	28.2	54.8	27.3	19.1	34.7
Inc[4] (%)	18.2	-	−40.5	−3.3	71.4	1632.3	−12.9	117.2	13.2

Subject Number	Age (yrs)	Gender	FEV_1 %Pred (%)	Short-time-scale ADC at t = 1 ms			Long-time-scale ADC at t = 1.5 s		
				SNR[1]	Mean ADC (cm^2/s)	%ADC -abn	SNR[2]	Mean ADC (cm^2/s)	%ADC -abn
r-value[#]	−0.51	-	1.00	−0.21	−0.56	−0.53	−0.03	−0.51	−0.51

FEV_1%pred is FEV_1%predict (percent-predicted forced expiratory volume in one second).

%ADC-abn is the percentage of the pixels whose ADC value was greater than the corresponding threshold (Mean + 2SD of all ADC values for the healthy group).

[1]SNR is the average SNR for the $b = 0$ image at the short-time scale.

[2]SNR is the average SNR for the first reference image at the long-time scale.

[3]CV is the coefficient of variations.

[4]Inc is the percentage increase compared with that of the healthy group.

[#]*r*-value is the *r*-value, correlated with the FEV_1%predict.